Biochemistry and Biophysics Reports 5 (2016) 346–352

Contents lists available at ScienceDirect

Biochemistry and Biophysics Reports

journal homepage: www.elsevier.com/locate/bbrep

Blocking the binding of WT1 to *bcl-2* promoter by G-quadruplex ligand SYUIQ-FM05

Yun-Xia Xiong [a,1], Ai-Chun Chen [a,1], Pei-Fen Yao [a], De-Ying Zeng [a], Yu-Jing Lu [b], Jia-Heng Tan [a], Zhi-Shu Huang [a], Tian-Miao Ou [a,*]

[a] School of Pharmaceutical Sciences, Sun Yat-sen University, Guangzhou 510006, PR China
[b] Faculty of Chemical Engineering and Light Industry, Guangdong University of Technology, Guangzhou 510006, PR China

ARTICLE INFO

Article history:
Received 21 July 2015
Received in revised form
21 December 2015
Accepted 29 December 2015
Available online 14 January 2016

Keywords:
WT1
Quindoline derivative
Bcl-2 gene
G-quadruplex forming sequence
Blocking binding

ABSTRACT

At present, *wt1*, a Wilms' tumor suppressor gene, is recognized as a critical regulator of tumorigenesis and a potential therapeutic target. WT1 shows the ability to regulate the transcription of *bcl-2* by binding to a GC-rich region in the promoter, which can then fold into a special DNA secondary structure called the G-quadruplex. This function merits the exploration of the effect of a G-quadruplex ligand on the binding and subsequent regulation of WT1 on the *bcl-2* promoter. In the present study, WT1 was found to bind to the double strand containing the G-quadruplex-forming sequence of the *bcl-2* promoter. However, the G-quadruplex ligand SYUIQ-FM05 effectively blocked this binding by interacting with the GC-rich sequence. Our new findings are significant in the exploration of new strategies to block WT1's transcriptional regulation for cancer-cell treatment.

1. Introduction

The human Wilms' tumor 1 (*wt1*) gene, located at chromosome 11p13, was originally identified as a tumor suppressor in Wilms' tumor in 1990 [1]. Because of its overexpression in hematologic malignancies and a variety of solid cancers, but not in the healthy adjacent tissues, *wt1* is currently considered as a potential oncogene [2,3] and a promising target for cancer therapy. *wt1* is a prognostic biomarker in uterine sarcoma [4] and in acute myeloid leukemia (AML) [5] because of its high correlation with cancer growth and relapse. The knockdown of WT1 effectively induces the apoptosis of leukemic cells [6] and inhibits malignant cell growth [7]. WT1 peptide vaccination of clinical patients with myeloid malignancies and several solid cancers has shown positive outcomes [8]. All of the substantial investigations implicate WT1 as a critical regulator of tumorigenesis and a potential therapeutic target.

The *wt1* gene encodes a zinc-finger transcription factor that can be translated into at least 36 isoforms by alternative mRNA splicing. All of these isoforms have four Cys2-His2 zinc fingers on their C-terminus [9]. The alternative splice sites at the end of exon 9 leads to the insertion of three amino acids (KTS) between zinc fingers 3 and 4, thereby forming two kinds of zinc-finger domains termed as ZF−KTS and ZF+KTS [10]. The ZF+KTS isoform usually binds to RNA and tends to function in the post-transcriptional regulatory processes [11], whereas the ZF−KTS isoform binds to DNA more strongly and is more active in transcriptional regulation [12]. By recognizing the consensus site 5′–GNGNGGGNG–3′, WT1 was reported as a transcriptional regulator that targets at least 137 genes. As such, WT1 plays important roles in cell processes, including cell differentiation, cell adhesion, apoptosis, angiogenesis, and immune function [13,14]. Interestingly, the GC-rich sites recognized by WT1 were reported to be remarkably associated with the potential G-quadruplex-forming motifs, which carry a signature motif of $G_{\geq 3}N_XG_{\geq 3}N_XG_{\geq 3}N_XG_{\geq 3}N_X$, in humans, chimpanzees, mice, and rats [15]. This observation implies the possible role of WT1 in transcriptional regulation through G-quadruplex elements. A well-known example is a 39 bp GC-rich element (Pu39) located upstream of the P1 promoter of the *bcl-2* oncogene (Fig. 1). In our study, we select a native sequence Pu59 from the *bcl-2* promoter; Pu39 sequence locates in the center of Pu59 and a 10-nucleotide flanking sequence was added on each side of Pu39. This region can be bound directly by the WT1 protein and plays an important role in the regulation of *bcl-2* gene transcription [16]. This guanine-rich sequence also has the potential to form a G-quadruplex structure and might cause the down-regulation of

Abbreviations: CD, circular dichroism; ChIP, chromatin immunoprecipitation; EMSA, electrophoretic mobility-shift assay; FRET, fluorescence resonance energy transfer; ITC, isothermal titration calorimetry; RT-PCR, reverse transcription polymerase chain reaction; FAM, 6-carboxyfluorescein; TAMRA, tetramethylrhodamine

* Corresponding author.
E-mail address: outianm@mail.sysu.edu.cn (T.-M. Ou).
[1] These authors contribute equally to this manuscript.

http://dx.doi.org/10.1016/j.bbrep.2015.12.014

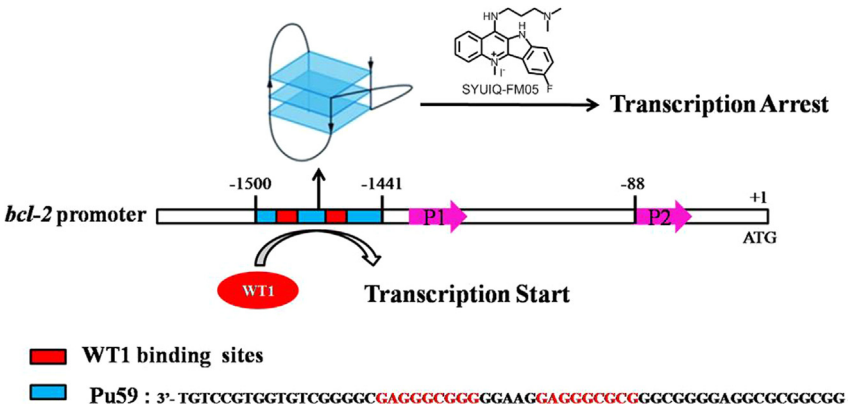

Fig. 1. WT1 binding sites in the *bcl-2* promoter and the G-quadruplex-forming sequence in the *bcl-2* promoter. Two conservative binding sites of WT1 exist in the Pu59 region (red region). The binding of WT1 to the *bcl-2* promoter will activate *bcl-2* transcription. The Pu59 region (blue region) in the *bcl-2* promoter *bcl-2* can form a G-quadruplex structure and be stabilized by compound SYUIQ-FM05. The resulting structure would lead to transcriptional arrest. The relationship among WT1, the Pu59 region, and the G-quadruplex ligand SYUIQ-FM05 will be further illustrated in this paper. (For interpretation of the references to color in this figure legend, the reader is referred to the web version of this article.)

bcl-2 transcription. Various G-quadruplex ligands have been reported possessing different functions, such as inhibition oncogenes' transcription, interfering with the telomere's function, and repressing tumor cell growth [17]. The high correlation between the WT1 binding sites and the G-quadruplex-forming site was noted. Hence, we explore whether or not WT1 can bind to the G-quadruplex structure. The second reason for our research is related to the positive roles that WT1 plays in leukemogenesis, in which it promotes tumor cell survival and affect clinical outcomes [18]. Moreover, *bcl-2* is reported to be transcriptionally upregulated by WT1 [19]. The coexpression of WT1 and BCL-2 is associated with response and long-term outcome of AMLs [20]. Therefore, we attempt to study the mechanism of the compound interfering with the transcriptional regulation of WT1.

In the present research, a variety of methods, including the electrophoretic mobility shift assay (EMSA), fluorescent studies, isothermal titration calorimetry (ITC), chromatin immunoprecipitation (Ch-IP), and circular dichroism (CD) were applied. For the first time, we demonstrated that WT1 cannot bind to the G-quadruplex structure. We identified a G-quadruplex ligand that could block WT1 binding by interaction with the GC-rich region containing the G-quadruplex-forming sequence in the promoter region of *bcl-2* gene. These new findings are significant in the development of new strategies to block WT1's transcriptional regulation for the treatment of leukemia cells.

2. Materials and methods

2.1. Materials

All chemicals were obtained from commercial sources. All oligomers were purchased from Invitrogen (China). The enzymes used for reverse transcription and PCR were purchased from TaKaRa (China), and the enzymes used for plasmid construction were purchased from Fermentas (USA). The compound was synthesized by our group as described previously [21] and was dissolved in dimethyl sulfoxide (DMSO) at the concentration of 10 mM as the stock solution. HL-60 (human promyelocytic leukemia cell lines) were obtained from the American Type Culture Collection and preserved at our laboratory. HL-60 cells were cultured in 1640 medium supplemented with 10% fetal bovine serum and 5% CO_2 at 37 °C. The antibodies employed in the study include WT1 polyclonal antibody (sc-192, Santa Cruz, CA, USA) and anti-rabbit IgG–horseradish peroxidase (#7074, Cell Signaling, MA, USA).

2.2. Plasmid construction and protein purification

Total mRNAs were isolated from the HL-60 cells using the RNAiso Plus reagent (TaKaRa, China) following the manufacturer's protocol. Then, 500 ng of total RNA was reverse transcribed in a total volume of 20 μL PCR mixture using the M-MLV reverse transcriptase (TaKaRa, China) and oligo $d(T)_{18}$ primer (TaKaRa, China). After reverse transcription, the cDNA was subjected to PCR for the amplification of the C-terminus of WT1 (amino acids 312–449) containing the four zinc fingers using primers ZF-A (5′–GGAATTCTCAAAGCGCCAGCTGGAG–3′) and ZF-S (5′–GAATTCCATATGTCGGCATCTGAGACCAG–3′). PCR was performed on a Bio-Rad T100 Thermal Cycler using Dreamtaq PCR kit (Thermo Scientific). The program proceeded as follows: initial denaturation at 95 °C for 10 min, followed by 30 cycles of denaturation, annealing, and extension (95 °C for 10 s, 58 °C for 30 s, and 72 °C for 1 min). The PCR products were verified using a 2% agarose gel. The PCR products digested by NdeI and EcoRI were inserted into a pET-28a (+) vector (Novagen, TX, USA) for pET28a-(ZF−KTS) plasmid construction.

All reconstructed plasmids were sequenced and confirmed by BLAST on NCBI.

The *E. coli* strain BL21 (DE3) cells were transformed with pET-28a-(ZF-KTS) plasmid for overexpression and purification of the recombinant protein. Cells were first grown at 37 °C in 0.2 l of LB medium containing kanamycin (50 ng/mL) to an OD600 of 0.6 before addition of 0.1 mM IPTG to induce protein expression. Cells were then grown at 15 °C for 18 h before harvested by centrifugation. Cell pellet was resuspended in 40 mL of start buffer (20 mM potassium phosphate, pH 7.4, 0.5 M NaCl) and lysed using a SCIENTZ-II D sonicator (SCIENTZ). The insoluble debris was removed by centrifugation, and the clear supernatant was used for protein purification after filtered through a 0.45 μm filter. Protein purification was carried out using the Hi-Trap column (GE Healthcare) according to the protocol supplied by the manufacturer. The purified protein fractions were filtered and stored in 20 mM Tris, 100 mM KCl, 1 mM DTT, and 10% glycerol, pH 7.4. The purified protein was identified by MALDI-TOF-TOF (Ultraflex TOF/TOF III) and Mascot Search and the purity were verified by SDS-polyacrylamide gel electrophoresis.

2.3. Electrophoretic mobility shift assay (EMSA)

The oligomers were diluted from stock solution to the indicated concentration in Tris–HCl buffer (10 mM, pH 7.4) with or without 100 mM KCl, and then annealed by heating to 95 °C for 5 min, and

gradually cooled to 25 °C. The sequence of the G-strand Pu59 was 5′-GGCGGCGCGGAGGGGCGGGCGCGGGAGGAAGG GGGCGGGACGGGGCTGTGGTGCCTGT-3′. The sequence of the mutant Pu59 was 5′- GGCGGCGCGGAGGGGCGGGCGCAAAAGGAAG GGGGCGGGAGCGG GGCTGTGGTGCCTGT-3′, whose binding site of WT-1 was changed. Py59 or mutPy59 were the complementary strands of Pu59 or mutant Pu59; ds59 or mutant ds59 was the annealed mixture of Pu59 and Py59, or mutant Pu59 and mutPy59, respectively. Subsequently, oligomers at indicated concentrations were incubated with the compound or recombinant protein at varying concentrations in EMSA binding buffer (20 mM HEPES, 2 mM DTT, 0.2 mg/mL BSA, 1% Triton X-100, 6% glycerol, pH 7.4) with or without 100 mM KCl for 1 h at 37 °C. Cold excess competitors (ds59 or mutant ds59) with 50-time amount of oligomers were added before incubation. The final volume was 20 μL. The reaction products were separated on 8% or 16% native polyacrylamide gels at 70 V for 4 h at 0 °C in the presence of ice-cooled 0.5 × TBE buffer. The gels were silver stained as described previously [22].

2.4. Chromatin immunoprecipitation (ch-IP) assay

Ch-IP was performed using the Agarose Ch-IP Kit (#26156, Pierce, USA) following the manufacturer's protocol. After 24 h of seeding about 2×10^6 HL-60 cells in a 10 cm^2 culture flask with or without the compound, the cells were fixed with 1% formaldehyde for 10 min and then lysed. Ch-IP-class WT1 primary antibody (sc-192, Santa Cruz, CA, USA) was used to immunoprecipitate chromatin in the HL-60 cells. Meanwhile, anti-rabbit IgG was used for mock immunoprecipitation, and the RNA polymerase II antibody provided by the kit was used as the positive control. Ch-IP was performed at 4 °C for 16 h, and the resulting immune complexes were collected using protein A magnetic beads provided by the kit. After extensive washing, the DNA was extracted from immunoprecipitated chromatin. Immunoprecipitated DNA samples were used to amplify different regions upstream the transcriptional starting site of *bcl-2*, or the other WT1 target gene *Pecam-1* with PCR primers (Table S1). The internal control glyceraldehyde 3-phosphate dehydrogenase (GAPDH) primers were provided by the kit. PCR was performed on a Bio-Rad T100 Thermal Cycler using Dreamtaq PCR kit (Thermo Scientific, EU). The program was as follows: initial denaturation at 95 °C for 10 min, followed by 30 cycles of denaturation, annealing, and extension (95 °C for 10 s, 58 °C for 30 s, and 72 °C for 1 min). The PCR products were separated on a 3% agarose gel.

2.5. UV–vis spectroscopic studies

Absorption spectral titration experiments were performed on a JASCO double beam recording spectrophotometer by maintaining a constant concentration of the compound (30 μM) with the oligomer at varying concentrations. Compound-DNA solutions were allowed to incubate for 5 min before the spectra were recorded. From the absorption data, the intrinsic binding constant, K_b, was determined using the following equation [23]:

$$[DNA]/(\varepsilon_a - \varepsilon_f) = [DNA]/(\varepsilon_b - \varepsilon_f) + 1/K_b(\varepsilon_b - \varepsilon_f) \quad (1)$$

where ε_a, ε_f, and ε_b are the apparent, free, and bound compound extinction coefficients, respectively. In the plots of $[DNA]/(\varepsilon_a - \varepsilon_f)$ versus [DNA], K_b was given the ratio of slope to the intercept.

2.6. Fluorescence spectroscopic studies

The 5′–FAM (6-carboxyfluorescein) and 3′–TAMRA (tetramethylrhodamine) dual-labeled *bcl-2* Mid oligomer (5′–GGGCGCGGGAGGAAGGGGGCGGG–3′) at a final concentration of 50 nM was incubated at 37 °C for 1 h with the purified WT1 protein at varying concentrations in fluorescence resonance energy transfer (FRET) binding buffer (20 mM HEPES, 2 mM dithiothreitol [DTT], 0.2 mg/mL bovine serum albumin [BSA], 1% Triton X-100, and 6% glycerol at pH 7.4) with or without 0.1 M KCl. The mixtures were applied to a Perkin-Elmer LS-55 luminescence spectrophotometer at 37 °C. A quartz cuvette with a 1 cm path length was used to obtain the spectra at 10 nm excitation and emission slit width. Fluorescence measurements were obtained at 480 nm excitation. The fluorescence-emission data points (from 500 nm to 650 nm) at each step were then recorded.

2.7. Circular dichroism (CD) spectroscopy

The oligomers at 5 μM final concentration were resuspended in CD binding buffer (10 mM Tris–HCl, and 0.1 M KCl at pH 7.4) with various amounts of the compound and incubated for 5 min at 25 °C. The CD spectra were documented on a Chirascan CD spectrophotometer (Applied Photo-physics, UK) at 25 °C. A quartz cuvette with a 4 mm path length was used in the process over a wavelength range of 230–400 nm at 1 nm bandwidth, 1 nm step size, and 0.5 s time per point. A buffer baseline was collected in the same cuvette and subtracted from the sample spectra. Final analysis of the data was performed using Origin 8.0 (OriginLab Corp.).

3. Results

3.1. WT1 binds to the GC-rich double-stranded region containing the G-quadruplex-forming sequence in the bcl-2 promoter

The high correlation between WT1 binding sites and G-quadruplex-forming site compelled us to explore the relationship between WT1 and the G-quadruplex-forming sequence in the *bcl-2* promoter region. The zinc-finger domain ZF−KTS is the key DNA recognition element of WT1 that binds to the *bcl-2* promoter and is effective in transcriptional regulation. Thus, we cloned the ZF−KTS domain and manipulated ZF−KTS in *E. coli* (Fig. S1). Pu59 was a G-rich DNA single strand of *bcl-2* and can form G-quadruplex structure, which was identified by using CD and ELISA (Fig. S2). As shown in Fig. S2A, the CD spectra of Pu59 exhibited typical parallel G-quadruplex signal with a positive peak at 262 nm and a negative peak at 240 nm. ELISA was also performed using G-quadruplex specific antibody BG4 [24]; the absorption at 450 nm could be used to identify the binding between BG4 and the nucleotide. As shown in Fig. S2B, Pu59 could significantly bind with BG4, indicating that this sequence could form G-quadruplex structure. Py59 was the corresponding C-rich complementary sequence and used to annealed with Pu59 to form the double-stranded structure. We found that ZF−KTS could bind to the double-stranded DNA in a dose-dependent manner (Fig. 2, line 1–4), but it did not bind to the Pu59 sequence (Fig. 2, line 7 and 8) or the Py59 sequence (Fig. 2, line 9 and 10). The addition of cold excess competitors was used to further identify the specificity of the binding. As shown in line 5 and 6 in Fig. 2, excess ds59 could reduce the amount of bound DNA while mutant ds59 could not show this effect, indicating that the binding between ZF-KTS and ds59 was specific. Moreover, the results from the FRET assay showed no change in the secondary structure of the G-rich sequence mid-G in the presence of WT1 (Fig. 3). Regardless of sequence, the G-quadruplex structure would still form in the presence of KCl or would not (in the absence of KCl). From the results of ELISA (Fig. S2B), the binding of BG4 to ds59 could still be detected while reduced comparing with the binding between BG4 and Pu59, implying G-quadruplex might form in this region. The results illustrated that ZF−KTS could only recognize and bind to

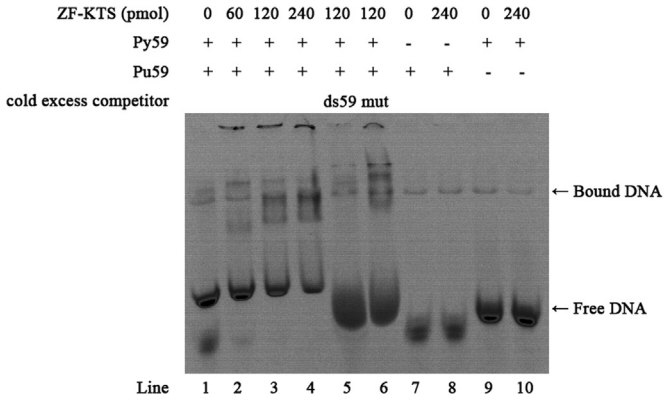

Fig. 2. EMSA for the binding of WT1 ZF−KTS to *bcl-2* double-stranded Pu59 without any competitor (lines 1–4) or with competitors (lines 5 and 6), Py59 (lines 7 and 8), and Pu59 (lines 9 and 10). Different oligomers (60 pmol) were incubated with the purified ZF−KTS protein at varying concentrations and separated by 16% native polyacrylamide gel electrophoresis (PAGE). Cold excess competitors (ds59 or mutant ds59) with 50-time amount of oligomers were added before incubation. The migration positions of the free and bound DNAs were indicated.

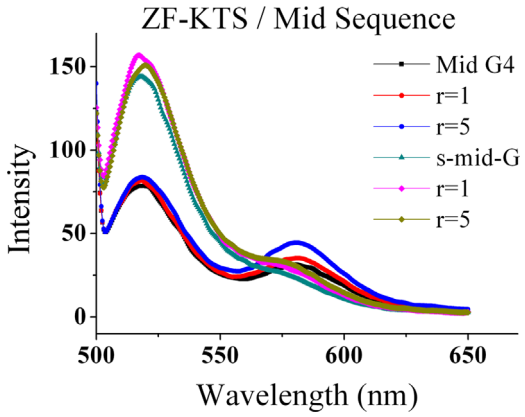

Fig. 3. FRET spectroscopy for the DNA secondary structure in the presence of WT1 zinc fingers. Mid G4: Mid sequence in 10 mM Tris–HCl buffer (pH 7.4) containing 100 mM KCl; s-mid-G: Mid sequence in 10 mM Tris–HCl buffer (pH 7.4). *r* represents the molar ratio of protein/DNA.

the double-stranded DNA instead of the single-stranded DNA in the *bcl-2* promoter, despite the secondary structure of the single-stranded DNA. However, whether the structural changes inside the WT1's binding sites, including the change in the duplex or the change in one of the strands, would influence WT1 binding remains unclear. We then performed the following experiments to address this issue.

3.2. Blocking WT1 binding with small molecule SYUIQ-FM05

To further verify the relationship between WT1 and the G-quadruplex structure, a quindoline derivative SYUIQ-FM05 was used, which was identified as a G-quadruplex stabilizer. The binding between ZF−KTS and ds59 DNA could be blocked by SYUIQ-FM05 in a dose-dependent manner (Fig. 4A, lines 2–5). On the other hand, this interfering effect could not be detected with the addition of ethidium bromide (EB), which is a conventional DNA-intercalating agent (Fig. 4A, lines 6–9). This result implies that SYUIQ-FM05 could specifically block the binding of WT1, and the interaction may not involve EB.

Based on the results, Ch-IP assay was conducted to identify the binding between WT1 and the *bcl-2* promoter at the cellular level. The human promyelocytic leukemia cell line (HL-60) with high WT1 expression was used. The primers that can amplify the GC-rich regions upstream of the transcription starting site were employed to detect the binding of WT1 to the GC-rich regions in the HL-60 cells. WT1 showed the most effective binding ability to the region from −1443 to −1636, which contains the G-quadruplex-forming sequence. No binding to other GC-rich regions was found (Fig. S3). Therefore, we chose this region for further investigation. As shown in Fig. 4B, the binding of WT1 weakened when cells were treated with 0.2 μM SYUIQ-FM05, but the WT1 expression level was maintained, as indicated by the Western blot (Fig. S4). The binding of RNA polymerase II to the *GAPDH* gene fragment, and the binding of WT1 to the other WT1 target gene *Pecam-1* [14], were not affected by the compound. This result indicated that the WT1 successfully bound to the region containing the G-quadruplex-forming sequence, and that SYUIQ-FM05 effectively blocked the binding of WT1 to the *bcl-2* promoter in the HL-60 cells.

3.3. SYUIQ-FM05 can effectively interact with the bcl-2 promoter Pu59 region

In a previous study, SYUIQ-FM05 was identified as a G-quadruplex ligand and exhibited strong binding affinity and stabilizing ability to the G-quadruplex structure in the *bcl-2* promoter [21]. To explore the reason underlying these repressive effects of SYUIQ-FM05 on WT1's binding to DNA, the binding abilities of SYUIQ-FM05 to ds59 or ZF−KTS were examined. UV titration was performed to investigate the binding properties of SYUIQ-FM05 to the Pu59 region (including Pu59, Py59, and ds59) and a random duplex DNA (Fig. 5). The spectral parameters of the UV titration assay are listed in Table 1. The binding constants obtained from UV titration indicated that SYUIQ-FM05 could effectively bind to Pu59 (G-quadruplex forming sequence) and ds59, with similar binding constants 1.83×10^7 and $1.23 \times 10^7\ M^{-1}$, respectively, but exhibited moderate binding ability to Py59 and random duplex. However, the ITC assay showed no obvious binding between ZF−KTS and SYUIQ-FM05 (Fig. S5). Therefore, although SYUIQ-FM05 was identified as a G-quadruplex ligand, it could still bind to ds59 DNA. The interaction with Pu59 region might be a major reason for blocking the binding of the WT1 zinc finger.

CD spectroscopy is useful in monitoring DNA conformational changes induced by the interaction of compounds. CD spectroscopy was used to further study the change in the secondary structure of the *bcl-2* Pu59 region induced by SYUIQ-FM05. The CD spectra of ds59 (Pu59 annealed with C-rich complementary strand sequence Py59) showed a double-strand signal with a positive peak at around 270 nm (Fig. 6A). The titration of SYUIQ-FM05 led to a decrease of this peak together with a slight shift to 265 nm in a dose-dependent manner, indicating that SYUIQ-FM05 could interact with ds59 and might change the conformation of the duplex oligomer. Remarkably, the positive peak on 265 nm was a typical signal of the G-quadruplex structure. EMSA, a convenient method to determine DNA conformational changes, was used to further identify the interaction between SYUIQ-FM05 and *bcl-2* ds59. As shown in Fig. 6B, the duplex-strand oligomer ds59 migrated slower and in a dose-dependent manner in the presence of SYUIQ-FM05. This finding may have been caused by the DNA conformational change. However, the ds59 did not migrate after the addition of EB, indicating that the migration was not due to DNA intercalation. Instead, it was due to the change in DNA conformation. We further identified whether this conformational change was due to the formation of G-quadruplex, however, the binding abilities of BG4 to both Pu59 and ds59 were similar after the addition of SYUIQ-FM05 (Fig. S2B).

4. Discussion

The high correlation between *wt1* and *bcl-2* in cancer cells and the prognostic relevance of the coexpression of both genes in AML

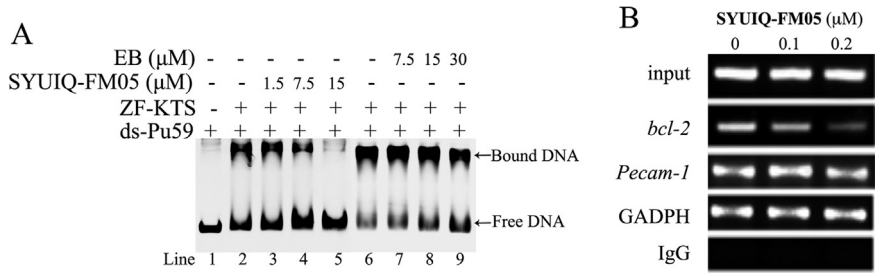

Fig. 4. Blocking of WT1 binding by SYUIQ-FM05. A. Different oligomers (1.5 μM) were incubated with 3 μM of the purified ZF−KTS protein and SYUIQ-FM05 at varying concentrations and separated by 8% PAGE. B. Ch-IP–PCR products of immunoprecipitation. HL-60 cells were treated with 0.2 μM SYUIQ-FM05 for 24 h, with DMSO used as control. The PCR product was amplified by primers occupying the −1443 to −1636 region of the *bcl-2* promoter. The binding of RNA polymerase II was used as the positive control, whereas the binding of IgG was used as the negative control. The binding of WT1 to the other WT1 target gene *Pecam-1* was also used as a positive control.

[20] compelled us to investigate the regulatory role of WT1 toward the *bcl-2* gene promoter by blocking WT1's binding by a small molecule. We identified a compound named SYUIQ-FM05 that can fulfill this blocking role. This study was the first attempt to interfere with WT1's binding to the *bcl-2* promoter by a G-quadruplex ligand. This is a new strategy for eliminating cancer cells besides the knockdown of WT1 or BCL-2 by antisense oligomers, which has shown good outcomes in AML treatment [6,25].

Considering that WT1 could bind to double-stranded conservative sites but not the corresponding G-quadruplex structure, a series of G-quadruplex ligands were screened with the objective of blocking the binding of WT1 to the *bcl-2* promoter (data not shown). Among these ligands, a quindoline derivative (SYUIQ-FM05) showed the strongest repression ability. Further studies showed that the repressive effect of SYUIQ-FM05 resulted from binding to the ds59 region but not the ZF−KTS. SYUIQ-FM05 reportedly stabilizes G-quadruplex structures in the Pu39 region, thereby down-regulating P1 promoter activity, reducing

Table 1
Spectral properties of UV titration.

DNA	λ_{max} (nm)		Hypochromism H (%)	Red shift ($\Delta\lambda$/nm)	Binding constant (K_b/M^{-1})
	Free	Bound			
Pu59	433	445	64.97	12	1.83×10^7
Py59	433	440	50.58	7	4.84×10^6
ds-Pu59	433	441	63.27	8	1.23×10^7
Random	433	440	45.31	7	2.57×10^6

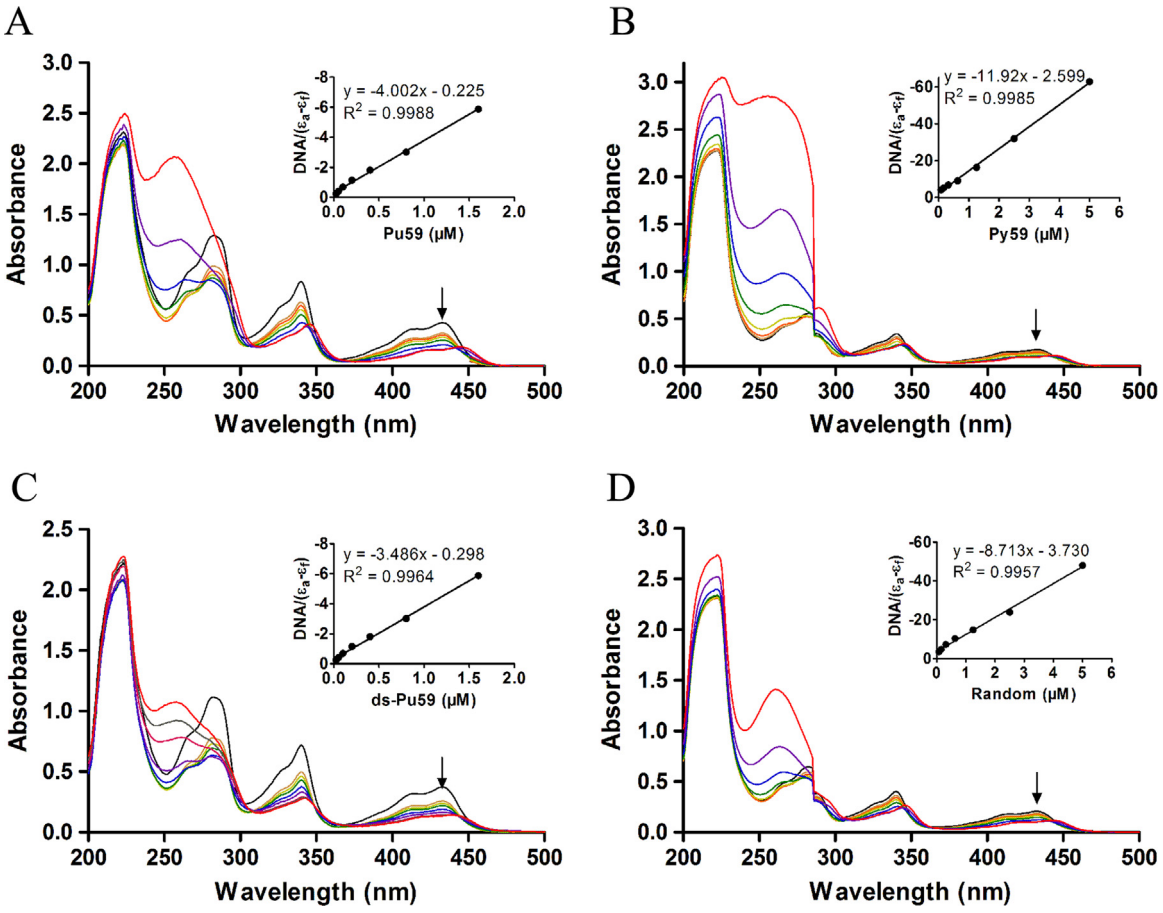

Fig. 5. UV–vis absorption spectra of 30 μM SYUIQ-FM05 in the presence of increasing amounts of DNA. [DNA]=0–5 μM. The arrow shows the spectral change upon increasing the DNA concentration. The inset is a plot of [DNA]/($\varepsilon_a - \varepsilon_f$) versus [DNA].

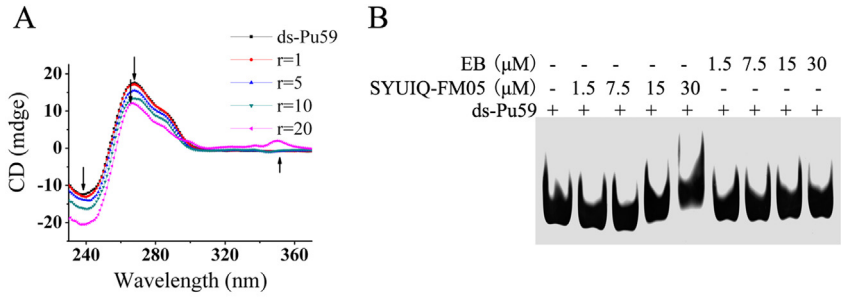

Fig. 6. The interaction between SYUIQ-FM05 with double-stranded Pu59. A. CD spectra of 5 μM double-stranded Pu59 induced by SYUIQ-FM05. The arrow indicates the spectral change with increasing compound concentration; *r* represents the molar ratio (compound/DNA). B. EMSA gel image for ds59 under different compound concentrations. A ds59 concentration of 1.5 μM was used in each sample, incubated with or without the compound at 37 °C for 1 h, and separated by 16% PAGE.

transcription/translation of the *bcl-2* gene, and finally leading to the apoptosis of HL-60 cells [26]. SYUIQ-FM05 was previously shown to possess a high binding affinity to the *bcl-2* G-quadruplex (with a K_D value of 32 nM) and moderate binding to duplex DNA (with a K_D value of 269 nM). These observations indicated that either the G-quadruplex or the duplex in the Pu59 region can be recognized by SYUIQ-FM05. When SYUIQ-FM05 interacted with ds59, CD and EMSA results showed that the conformation of ds59 was altered. However, the specific secondary structure remained unknown. Overall, WT1 binding may be repressed by SYUIQ-FM05 either by stabilizing the G-quadruplex or interacting with the double strand Pu59. Given the effective interaction between SYUIQ-FM05 and the GC-rich double-strand region, further investigations on whether SYUIQ-FM05 could block the binding of other zinc finger transcription factors, such as SP1, MAZ and ZF5 are needed. We were not able to identify the kinds of secondary structure induced by SYUIQ-FM05 because we were limited by experimental technique.

In conclusion, our results showed that SYUIQ-FM05 could interact with the double-stranded Pu59 region of *bcl-2* and change the DNA conformation to block the binding of WT1. This phenomenon may also be another reason for the down-regulated *bcl-2* expression and apoptosis of HL-60 cells. Blocking the binding of WT1 is a promising new approach for drug design in cancer treatment.

Acknowledgments

We thank Professor S. Balasubramanian and J. McCafferty from University of Cambridge giving the BG4 antibody for this research. We thank the National Natural Science Foundation of China (Grants 21372263, 91213302, and 81330077), the Fundamental Research Funds for the Central Universities (Grant 11ykzd04), the Zhujiang Nova Program (Grant 2011J2200075), and the Foundation for Distinguished Young Talents in Higher Education of Guangdong (Grant Yq2013002) for the financial support to this study.

Appendix A. Supplementary material

Supplementary data associated with this article can be found in the online version at http://dx.doi.org/10.1016/j.bbrep.2015.12.014.

References

[1] K.M. Call, T. Glaser, C.Y. Ito, A.J. Buckler, J. Pelletier, D.A. Haber, E.A. Rose, A. Kral, H. Yeger, W.H. Lewis, et al., Isolation and characterization of a zinc finger polypeptide gene at the human chromosome 11 Wilms' tumor locus, Cell 60 (1990) 509–520.
[2] L. Yang, Y. Han, F. Suarez Saiz, M.D. Minden, A tumor suppressor and oncogene: the WT1 story, Leukemia 21 (2007) 868–876.
[3] X.W. Qi, F. Zhang, H. Wu, J.L. Liu, B.G. Zong, C. Xu, J. Jiang, Wilms' tumor 1 (WT1) expression and prognosis in solid cancer patients: a systematic review and meta-analysis, Sci. Rep. 5 (2015) 8924.
[4] A. Coosemans, B. Van Calster, G. Verbist, P. Moerman, I. Vergote, S.W. Van Gool, F. Amant, Wilms tumor gene 1 (WT1) is a prognostic marker in high-grade uterine sarcoma, Int. J. Gynecol. Cancer 21 (2011) 302–308.
[5] Y. Yi-Ning, W. Xiao-Rui, Z. Chu-Xian, W. Chun, Q. You-Wen, Prognostic significance of diagnosed WT1 level in acute myeloid leukemia: a meta-analysis, Ann. Hematol. 94 (2015) 929–938.
[6] W. Glienke, L. Maute, U. Koehl, R. Esser, E. Milz, L. Bergmann, Effective treatment of leukemic cell lines with wt1 siRNA, Leukemia 21 (2007) 2164–2170.
[7] N. Tatsumi, Y. Oji, N. Tsuji, A. Tsuda, M. Higashio, S. Aoyagi, I. Fukuda, K. Ito, J. Nakamura, S. Takashima, Y. Kitamura, S. Miyai, T. Jomgeow, Z. Li, T. Shirakata, S. Nishida, A. Tsuboi, Y. Oka, H. Sugiyama, Wilms' tumor gene WT1-shRNA as a potent apoptosis-inducing agent for solid tumors, Int. J. Oncol. 32 (2008) 701–711.
[8] A. Di Stasi, A.M. Jimenez, K. Minagawa, M. Al-Obaidi, K. Rezvani, Review of the results of WT1 peptide vaccination strategies for myelodysplastic syndromes and acute myeloid leukemia from nine different studies, Front. Immunol. 6 (2015) 36.
[9] I. Lindstedt, M.A. Lindgren, E. Andersson, W. Engstrom, The WT1 gene–its role in tumourigenesis and prospects for immunotherapeutic advances, In Vivo 28 (2014) 675–681.
[10] D.A. Haber, R.L. Sohn, A.J. Buckler, J. Pelletier, K.M. Call, D.E. Housman, Alternative splicing and genomic structure of the Wilms tumor gene WT1, Proc. Natl. Acad. Sci. USA 88 (1991) 9618–9622.
[11] T.C. Weiss, P.J. Romaniuk, Contribution of individual amino acids to the RNA binding activity of the Wilms' tumor suppressor protein WT1, Biochemistry 48 (2009) 148–155.
[12] Y. Han, S. San-Marina, L. Yang, H. Khoury, M.D. Minden, The zinc finger domain of Wilms' tumor 1 suppressor gene (WT1) behaves as a dominant negative, leading to abrogation of WT1 oncogenic potential in breast cancer cells, Breast Cancer Res. 9 (2007) R43.
[13] E. Toska, S.G. Roberts, Mechanisms of transcriptional regulation by WT1 (Wilms' tumour 1), Biochem. J. 461 (2014) 15–32.
[14] K.D. Wagner, J. Cherfils-Vicini, N. Hosen, P. Hohenstein, E. Gilson, N.D. Hastie, J. F. Michiels, N. Wagner, The Wilms' tumour suppressor Wt1 is a major regulator of tumour angiogenesis and progression, Nat. Commun. 5 (2014) 5852.
[15] P. Kumar, V.K. Yadav, A. Baral, P. Kumar, D. Saha, S. Chowdhury, Zinc-finger transcription factors are associated with guanine quadruplex motifs in human, chimpanzee, mouse and rat promoters genome-wide, Nucleic Acids Res. 39 (2011) 8005–8016.
[16] C. Heckman, E. Mochon, M. Arcinas, L.M. Boxer, The WT1 protein is a negative regulator of the normal bcl-2 allele in t(14;18) lymphomas, J. Biol. Chem. 272 (1997) 19609–19614.
[17] Y. Yan, J. Tan, T. Ou, Z. Huang, L. Gu, DNA G-quadruplex binders: a patent review, Expert. Opin. Ther. Pat. 23 (2013) 1495–1509.
[18] Z. Ujj, G. Buglyo, M. Udvardy, G. Vargha, S. Biro, L. Rejto, WT1 overexpression affecting clinical outcome in non-hodgkin lymphomas and adult acute lymphoblastic leukemia, Pathol. Oncol. Res. 20 (2014) 565–570.
[19] M.W. Mayo, C.Y. Wang, S.S. Drouin, L.V. Madrid, A.F. Marshall, J.C. Reed, B. E. Weissman, A.S. Baldwin, WT1 modulates apoptosis by transcriptionally upregulating the bcl-2 proto-oncogene, EMBO J. 18 (1999) 3990–4003.
[20] T. Karakas, C.C. Miething, U. Maurer, E. Weidmann, H. Ackermann, D. Hoelzer, L. Bergmann, The coexpression of the apoptosis-related genes bcl-2 and wt1 in predicting survival in adult acute myeloid leukemia, Leukemia 16 (2002) 846–854.
[21] Y.J. Lu, T.M. Ou, J.H. Tan, J.Q. Hou, W.Y. Shao, D. Peng, N. Sun, X.D. Wang, W. B. Wu, X.Z. Bu, Z.S. Huang, D.L. Ma, K.Y. Wong, L.Q. Gu, 5-N-methylated quindoline derivatives as telomeric g-quadruplex stabilizing ligands: effects of 5-N positive charge on quadruplex binding affinity and cell proliferation, J. Med. Chem. 51 (2008) 6381–6392.
[22] B.J. Bassam, P.M. Gresshoff, Silver staining DNA in polyacrylamide gels, Nat. Protoc. 2 (2007) 2649–2654.

[23] A. Wolfe, G.H. Shimer Jr., T. Meehan, Polycyclic aromatic hydrocarbons physically intercalate into duplex regions of denatured DNA, Biochemistry 26 (1987) 6392–6396.
[24] G. Biffi, D. Tannahill, J. McCafferty, S. Balasubramanian, Quantitative visualizatio of DNA G-quadurplex structures in human cells, Nat. Chem. 5 (2013) 182–186.
[25] R.J. Klasa, A.M. Gillum, R.E. Klem, S.R. Frankel, Oblimersen Bcl-2 antisense: facilitating apoptosis in anticancer treatment, Antisense Nucleic Acid Drug Dev. 12 (2002) 193–213.
[26] X.D. Wang, T.M. Ou, Y.J. Lu, Z. Li, Z. Xu, C. Xi, J.H. Tan, S.L. Huang, L.K. An, D. Li, L. Q. Gu, Z.S. Huang, Turning off transcription of the bcl-2 gene by stabilizing the bcl-2 promoter quadruplex with quindoline derivatives, J. Med. Chem. 53 (2010) 4390–4398.